Discrimination between local earthquakes and quarry blasts in the Vértes Mountains, Hungary

Márta Kiszely[1], Bálint Süle[1], Péter Mónus, István Bondár[2]

[1]ELRN, Institute of Earth Physics and Space Science, Kövesligethy Radó Seismological Observatory Meredek utca 18, Budapest 1112, Hungary

[2]ELRN, Institute for Geological and Geochemical Research, Research Centre for Astronomy and Earth Sciences

Kiszely.Marta@epss.hu

Abstract

We present our analysis of the characteristics of the waveforms of earthquakes and quarry blasts that occurred within extreme local-distance (< 25 km) of Csókakő (CSKK) station in the Vértes Hills, Hungary. Our motivation was to determine the linear discrimination line between the earthquake and explosion populations. CSKK is located in the Mór Graben, a seismically relatively active region, and also characterized by significant mining activity. Contamination of earthquake catalogues with anthropogenic events largely complicates seismotectonic interpretation. It is especially true for relatively low seismicity areas, such as Hungary where more than 50% of the recorded seismicity is attributed to anthropogenic events. We tested the effectiveness of the maximum P/S amplitude ratios in various frequency bands. Because most of the quarry blasts are carried out by ripple-fire technology, we also computed spectrograms and examined the spectral ratio between low and high frequencies and the steepness of spectra. We found that earthquakes and quarry blasts are best separated by the linear discrimination that combines the amplitude ratios and the different spectral ratios.

Keywords Quarry blasts · Discrimination · Linear Discriminant Function · Earthquakes

Introduction

The development of methodologies to distinguish natural seismicity from man-made events began during the cold war for monitoring nuclear tests. Seismic discrimination became an important component of national verification regimes of various nuclear treaties. Nowadays the new challenge is to develop the capability to discriminate between chemical explosions, quarry blasts and small earthquakes at local distances. However, relatively little attention has focused on discriminatory methods for very local distances (< 20 km), the range at which the smallest events are recorded and

may not be seen at more distant stations. In this paper we focus on discrimination techniques that can be applied at the closest range from the source.

Seismological event discrimination methods typically have been applied to distinguish explosions from tectonic events and to analyze their characteristics using the theoretical differences between the source mechanisms and epicentral depths. The source mechanism of tectonic earthquakes consists of shear dislocation, so S-wave energy dominates, whilst in the case of explosions isotropic pressure pulse occurs, and the P-wave and fundamental mode Rayleigh waves Rg energy dominates. For shallow sources, Rg is often the largest amplitude seismic phase at local distances. The ratio of the body wave and surface wave magnitudes (mb:Ms) is one of the most successful discriminator between natural events and nuclear explosion (Douglas at al. 1974; Pomeroy et al. 1982). Whereas it is applicable to teleseismic distances, at local and near-regional distances its discriminating power diminishes.

At local and regional distances fundamental mode Rayleigh waves with periods between about 0.6 and 2 Hz (Rg) are often observed on seismograms of explosions and very shallow depth earthquakes. The Rg phase is particularly prominent on seismograms of quarry blasts. Sources deeper than about 4 km would not be expected to generate strong Rg signals at these periods; and so, if Rg can be clearly identified on a seismogram, the source is most likely very shallow. Observed Rg waves can, therefore, be used to discriminate very shallow-focus events from deeper events, provided that Rg can be identified and distinguished from other phases. Kafka (1990) used successfully Rg (filtered 0.66-2 Hz) as a depth indicator for regional events.

However, the discrimination parameters are region-dependent. Kim et al. (1994) have shown that ripple firing results in an enrichment of high-frequency S waves and efficient excitation of the Rg phase. They have found an azimuthal dependence of P-wave amplitude associated with the orientation of the path with respect to local topography (ridges, benches) in which the shots are emplaced. A large number of studies have identified short period discriminators for particular regions. The most popular discriminator is the amplitude peak ratio of the S to P waves versus the logarithm amplitude peak of the S wave in the time domain of the seismogram (Baumgardt and Young 1990; Taylor et al. 1988; Wüster 1993; Horosan et al. 2009; Yılmaz et al. 2013). Allmann et al. (2008) also compared P- and S-wave amplitudes and have found modestly smaller average S amplitudes for the explosions compared to the earthquakes occurred in southern California. Zeiler & Velasco (2009) developed local to near-regional (0–200 km) amplitude discriminants using earthquakes, single-fired explosions, and delayed-fired explosions. They found that lithology, local site effects, and large-scale geologic features control most of the variability in the amplitude measurements. Kekovali et al. (2012) investigated regional seismic events ($2.3 \leq Md(duration) \leq 3.0$

using picking maximum amplitudes of Pg and Sg waves for the vertical component of the velocity seismograms, and found considerable overlap in earthquake and mining blast populations.

The spectral analysis of the different parameters included the examination of modified spectrum caused by the ripple firing blasting technique and the study of the binary spectrum and spectral scalloping (Gitterman & Eck 1993). The spectral representation of some wave groups, spectral ratios of seismic phases and spectrograms have been used as discriminants for different seismic events (Hedlin et al. 1989; 1998; Budakoglu & Horosan 2019). The spectral slope and the spectral ratio between the lower and higher frequency ranges was proved to be successful, so was the ratio of the average and the maximum value of the spectrum at a given frequency range (Kekovali et al. 2012). Musil & Plesinger (1996) presented the application of artificial neural nets to discriminate microearthquakes from quarry/mining blasts in the West Bohemia earthquake swarm region.

Linear discriminant functions are used by researchers to classify earthquakes and quarry blasts. Kintner at al. (2020) explored the effectiveness of local-distance (here considered less than 200 km epicentral distance) seismic discriminants to distinguish between surface mine blasts, single-shot borehole explosions, and earthquakes in the Bighorn Mountains region, Wyoming. Vargas at al. (2017) defined a discriminant function for Spanish stations' training dataset by a linear combination of the different parameters. They measured the maximum Lg amplitude/maximum P amplitude ratio in time domain, the logarithms of Lg amplitude ratios 1–2/6–8 Hz and 1–2/7–9 Hz, and calculated the frequency domain spectral peaks and slopes: P and Lg spectral decay and spectral variance. Lg phase is a wave group observed at regional distances and caused by superposition of multiple S-wave reverberations and SV to P and/or P to SV conversions inside the whole crust, and the Pg/Lg spectral ratio is often used parameter for discrimination. Their results show that Lg spectral variance plays a major role in single-station discriminant functions, as well as the logarithm of Lg amplitude ratio in 1–2/7–9 Hz and the logarithm of Lg amplitude ratio in 1–2/6–8 Hz. Budakoğlu & Horosan (2018) performed linear discriminant function to classify seismic events occurring in the Sakarya region at the North Anatolian Fault Zone. Time and frequency variant parameters, maximum S wave and maximum P wave amplitude ratio (S/P), the spectral ratio, maximum frequency and total signal duration of the waveform were used for their discrimination analyses.

Wiemer and Baer (2000), Gulia (2010), and Kekovali et al. (2011) used daytime hours to discriminate explosions from earthquakes. Kiszely & Győri (2015) analyzed the separation of quarry blasts from the aftershock sequence of the ML 4.5 Oroszlány (Hungary) earthquake, occurred on January 29, 2011. They found that quarry blasts preferably took place during daytime between 8 and 12 hours, but the diurnal distribution of $M_L > 0.2$ earthquakes of Vértes Mountains

region between the years 2011 and 2012 showed a small maximum between 12 and 16 hours. This midday peak may have been caused by misclassified explosions.

Our objective is to find the best single station discrimination method and parameters between earthquakes and quarry blasts in Vértes Mountains, Hungary, a region that regularly sees low-magnitude earthquake swarms as well as almost continuous activity at several quarries that produce ML < 2 events. Our data set contains events that were recorded at CSKK station between January 2017 and July 2019 as well as events from the aftershock sequence of the 29 January 2011 M_L 4.5 earthquake that occurred near Oroszlány, 13 km from CSKK. Thus, the training, validation and test data sets consist of 197 quarry blasts and 147 earthquakes, altogether 344 events,

We tested the effectiveness of the maximum P/S amplitude ratios using different frequency filtered waveforms. Because most of the quarry blasts were carried out by ripple-fire technology, we computed spectrograms and examined the spectral ratio (SR) between low and high frequencies and the steepness of spectra.

Tectonics and seismicity

The Pannonian Basin is located between the seismically active Mediterranean region and the nearly aseismic East European platform. Its tectonics is determined by the counterclockwise rotation of the Adria microplate and the north-northeast directed movement originating from the rotation (Bada et al, 2007) The seismicity of Hungary can be characterized as moderate and the distribution of earthquake epicenters shows a rather scattered pattern. The Hungarian National Seismological Network (HU, doi:10.14470/UH028726), operated by the Kövesligethy Radó Seismological Observatory, ELRN, Institute of Earth Physics and Space Science operates 15 permanent and 11 temporary broadband seismological stations that densely covers the country and is able to detect hundreds of seismic events annually. Nowadays approximately two third of the seismically recorded events are anthropogenic events, such as quarry blasts and mine explosions. The discrimination problem is particularly challenging because in Hungary small tectonic earthquakes occur together with small quarry blasts. The yellow rectangle in **Figure 1a** shows our region of interest, the Mór Graben and the Vértes Mountains. **Figure 1b** shows the event locations (HNSB, Gráczer et al., 2018, 2019). In the case of Magyaralmás blasts and other small earthquakes we supplemented our data from the bulletin of Tóth et al., (2018, 2019, 2020). Since the earthquake and quarry blast locations overlap, and may suffer from several kilometer location errors, discrimination based on the hypocenter parameters alone could not be used. Most earthquakes were recorded by only the three closest stations. Several quarry blasts were detected only by the CSKK stations. These were only used in the analysis if they were confirmed by mine operators. The Oroszlány aftershocks were relocated with a global 3D Velocity Model (Bondár et al 2018).

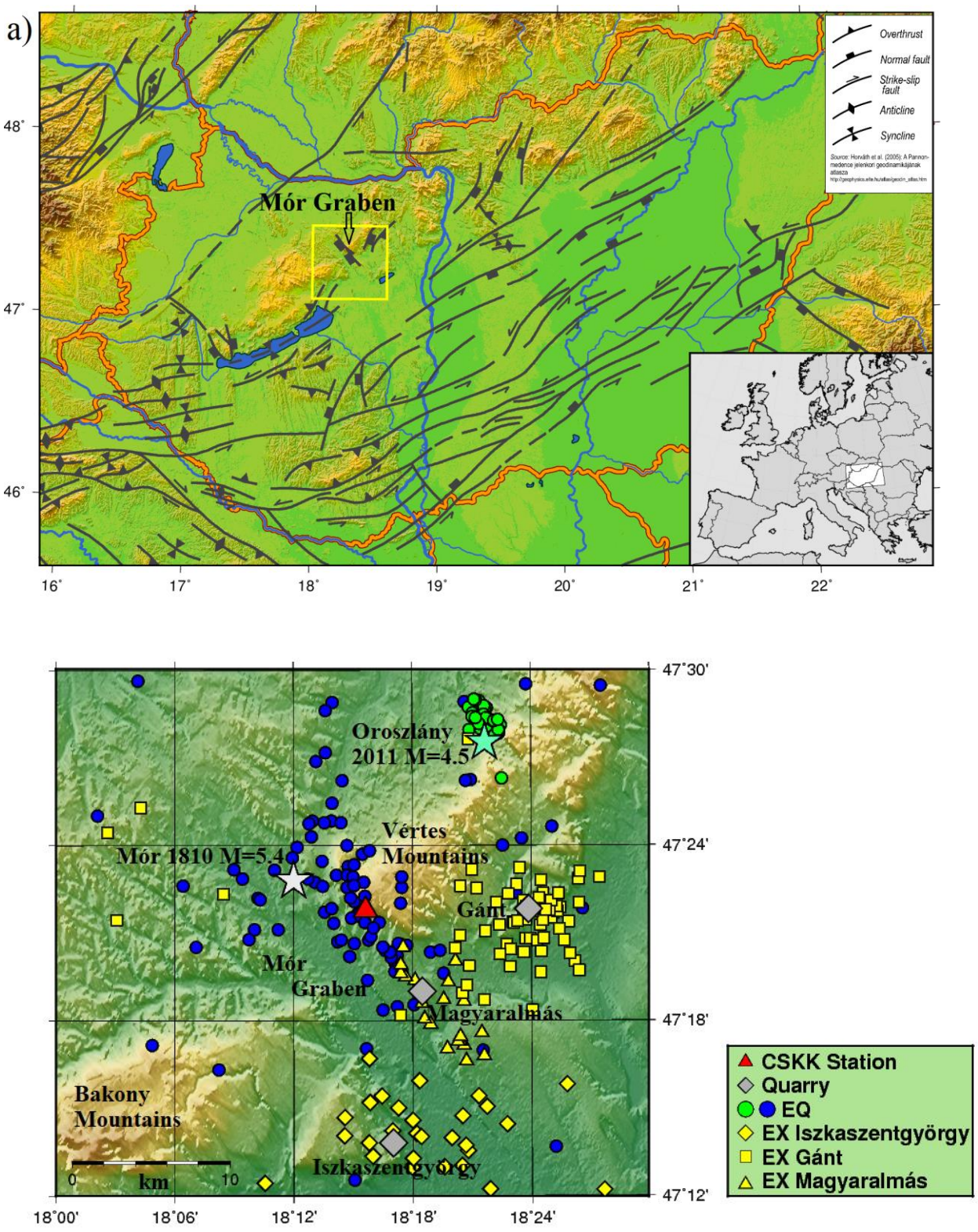

Figure 1. a) The investigated area in Hungary is marked with a yellow square (after http://geophysics.elte.hu/atlas/geodin_atlas.htm). Major faults in the Pannonian Basin are also indicated. b) Event locations. Blue circles indicate the earthquakes occurred between 2017.01 and 2019.07. The green star shows the mainshock M_L=4.5 Oroszlany, and the green circles its aftershocks. The white star represents the epicenter of Mór 1810.01.14 M_L=5.4 earthquake. Grey diamonds indicate quarry locations. The yellow symbols represent the calculated epicenters of the Magyaralmás (triangle), Gánt (square) and Iszkaszentgyörgy (diamond) quarries.

The Mór Graben is a curved, slightly segmented fault zone, which is expressed in the morphology as a steep slope of 100–250 m height. The total displacement of the fault can reach 1000–1200 m, taking into account borehole and seismic reflection data. The Mór Fault was active in the Oligocene and in several Miocene–Pliocene phases, and geological evidence support the neotectonic activity of the area. (Budai et al., 2008; Fodor et al. 2013). Joó and Csepregi (2007) reported 4.9 and 2.7 mm/a vertical uplift at the eastern and western sides of Mór Graben, between 1991 and 2005, respectively. The M5.4 Mór earthquake in 1810 was one of the largest earthquakes in Hungary. The Mór Graben is still active, as preliminary results from a temporary deployment of three stations in the vicinity of the CSKK station show that earthquakes, doublets and sometimes swarms with M < 1 can be regularly observed in the Mór Graben (Tóth et al (2018, 2019, 2020)..

Data: training, validation and test datasets

To build a training, validation and test data set, data of seismic events were collected from the Hungarian National Seismological Bulletin for 2017 and 2018 (HNSB, Gráczer et al., 2018, 2019), completed with the preliminary event list for 2019, which is not yet published at the time of writing. The event identification (earthquake or suspected explosion) was made by its origin time and location. **Figure 2** shows the temporal distribution of seismicity as a function of hours of the day and the day of the week. Quarry blasts typically occur between 6 and 11 am (UTC). However, due to the overlap between explosions and earthquakes, time of the day values provide insufficient information to classify earthquakes and quarry blasts.

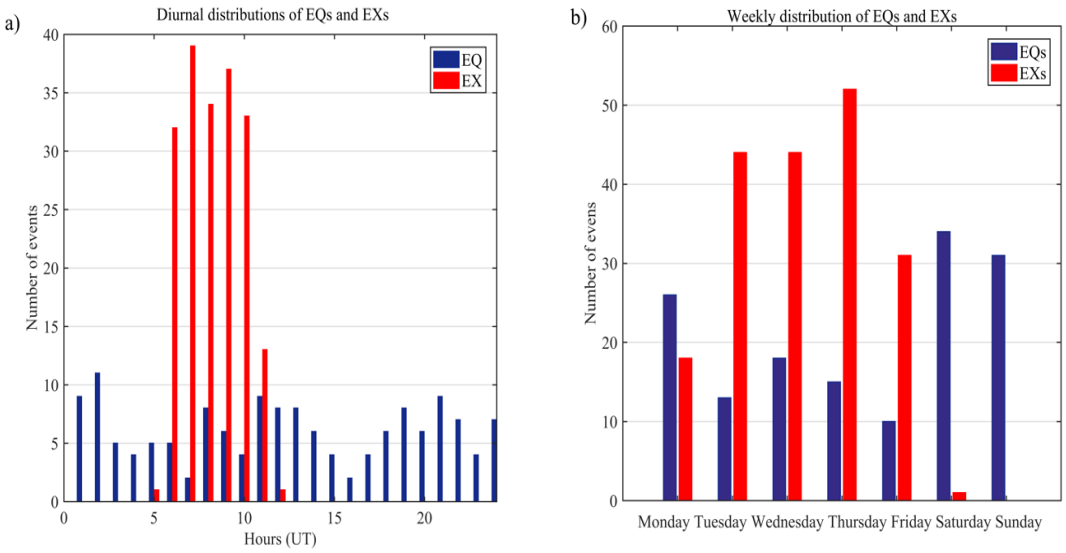

Figure 2. a) Diurnal and b) weekly distributions of earthquakes and quarry blasts in the investigated area. Explosions occur in the morning hours, and on workdays. There is still a significant overlap with earthquakes.

In several cases we have received the list of the date of explosions from the mining districts. However, the data provision from the quarries is often deficient, but some of the explosions are

considered ground truth. The magnitude of quarry blasts ranges between M_L 0.8-1.8, and for earthquakes between M_L 0.2-4.5. The largest event was the M_L 4.5 mainshock of the Oroszlány earthquake occurred on January 29, 2011 17:41:38, 47.480°N, 18.361°E at 9 km depth. **Table 1** shows that the data sets contain altogether 147 earthquakes and 197 explosions for the seismic discrimination at CSKK. We divided the data set to training (60% of the events), validation (20%) and test (20%) data sets. The test data set consists of 29 earthquakes and 37 confirmed quarry blasts.

Table 1. The characteristics of different groups of analyzed data

Events	Time interval	Number of events	Distance from CSKK
EQs - Oroszlány aftershocks	2011.01 - 2011.04	46	9-17 km
EQs - in Mór Graben	2017.01 - 2019.07	101	0.2-29 km
EXs - Gánt quarry	2017.01 - 2019.07	118	10.4 km
EXs - Iszkaszentgyörgy quarry	2017.01 - 2019.07	61	15.5 km
EXs - Magyaralmás quarry	2017.01 - 2019.07	18	6.5 km

The spectral features of earthquake and quarry blast signals are significantly different. **Figure 3** shows the vertical component seismograms and spectrograms of an earthquake and a quarry blast. The epicenter of this earthquake is 22 km from CSKK (M_L=1.6) and richer at high frequencies. The quarry blast is a typical event from the Gánt quarry (M_L=1.5), 10 km away from CSKK. Because of the ripple fire source, in most of the cases the explosions generate Rg phase.

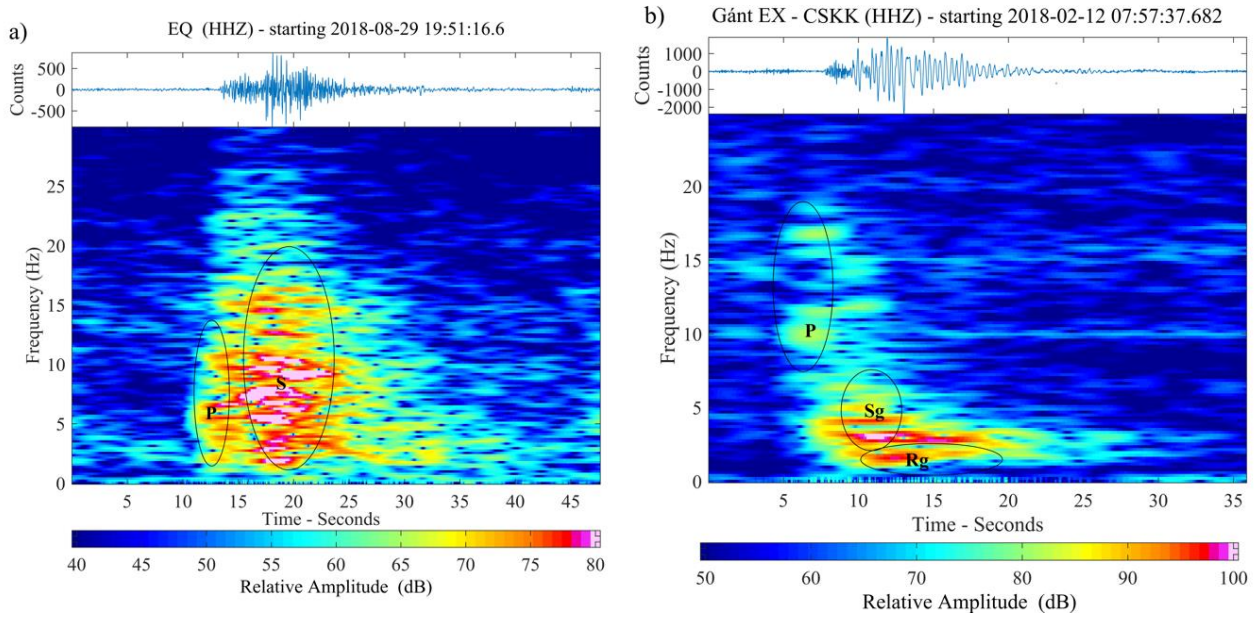

Figure 3. Example of the spectrogram for a) an earthquake and b) quarry blast at Gánt quarry. The spectrograms were computed from the vertical component of the waveforms. Purple, red, and light green colors indicate high energy contents, whereas dark green and turquoise colors indicate low energy contents.

Figure 4 shows the spectral features of quarry blasts originated from Magyaralmás and Iszkaszentgyörgy quarries. Note that infrasonic wave arrivals from these quarry blasts are regularly recorded at CSKK station at about 80% of the time, because the station is in the direct line of sight of these quarries.

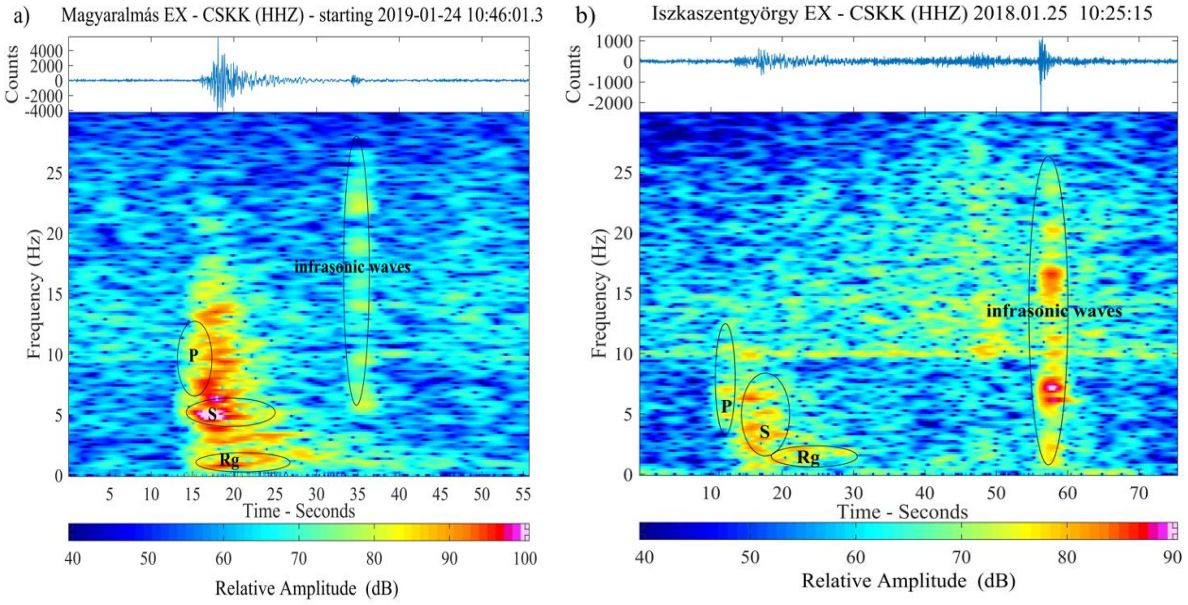

Figure 4. Example of spectrograms for quarry blasts from a) Magyaralmás and b) Iszkaszentgyörgy.

Figure 5 shows the power spectra of the earthquake and quarry blast for the events in **Figure 3**. The blasts were carried out by the ripple-fire technology (delay time was about 100 ms) which modulates the spectra of blasts so its spectra between 1-10 Hz are richer and the steepness of spectra proved smaller or negative compared to the spectra of earthquakes. The steepness of log amplitude spectra shows different slopes between 1-10 Hz (black line).

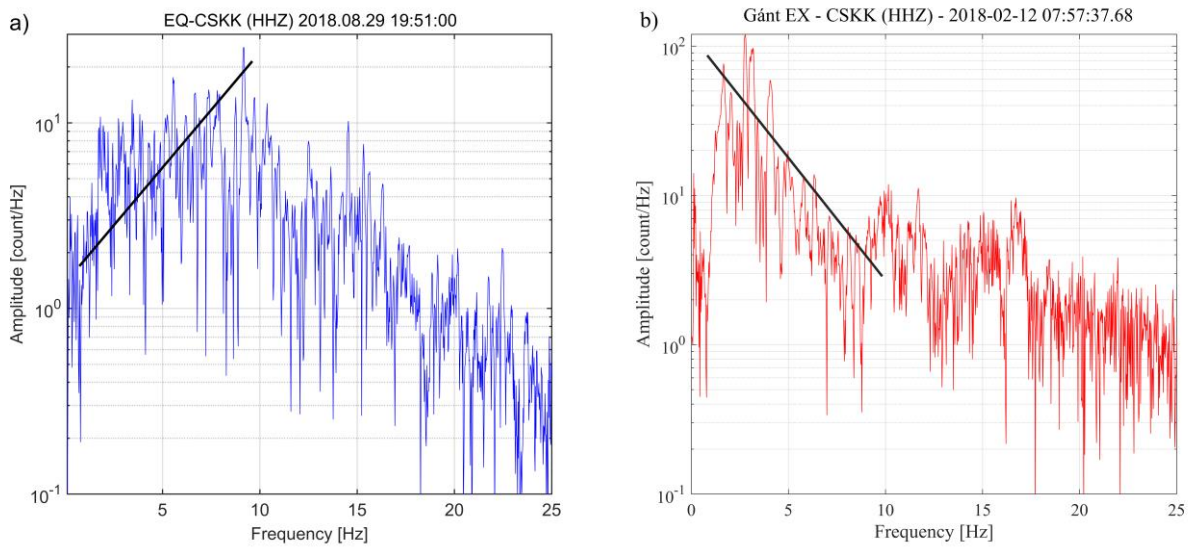

Figure 5. Amplitude spectra for a) an earthquake and b) a quarry blast at Gánt. The steepness of log power spectra shows an opposite slope between 1-10 Hz (black line).

Methods: Linear discrimination

We used three different approaches for the discrimination analysis between quarry blasts and earthquakes in the Vértes Mountains, Hungary. First, we obtained the different maximum phase amplitude ratios from the waveform analysis and performed a linear discrimination analysis using MATLAB tools. We also performed linear discrimination analysis on spectral amplitude ratios and spectral steepness. Finally, we combined the spectral and waveform analysis parameters together. Each seismogram was processed by removing the instrument response, the mean and trend and followed by tapering and filtering with a two-pole, two-pass Butterworth band-pass filter.

Once the linear discrimination functions were determined from the training data set, we applied them to the validation data set and measured the success of discrimination by constructing the confusion matrix of true and false positives and negatives.

Maximum phase amplitude ratios

Since the epicentral distances are less then 25 km, the temporal separation of Rg and Sg phases is small and the errors in the catalog event origin time or location are large enough to shift the Rg or Sg phase out of the narrowly defined time 2-6 s long windows. Therefore, we used the maximum amplitudes measured at different frequency bands and channels. The time and amplitude picking were performed with the help of the software package SeisGram2K (Lomax et al 2009).

Figure 6 illustrates our methodology. We measure the P and S coda maximum amplitudes in 6–8 Hz frequency band on channels HHZ and HHN, respectively. We measure the Rg maximum amplitude between 0.5- 2 Hz on the HHZ channel.

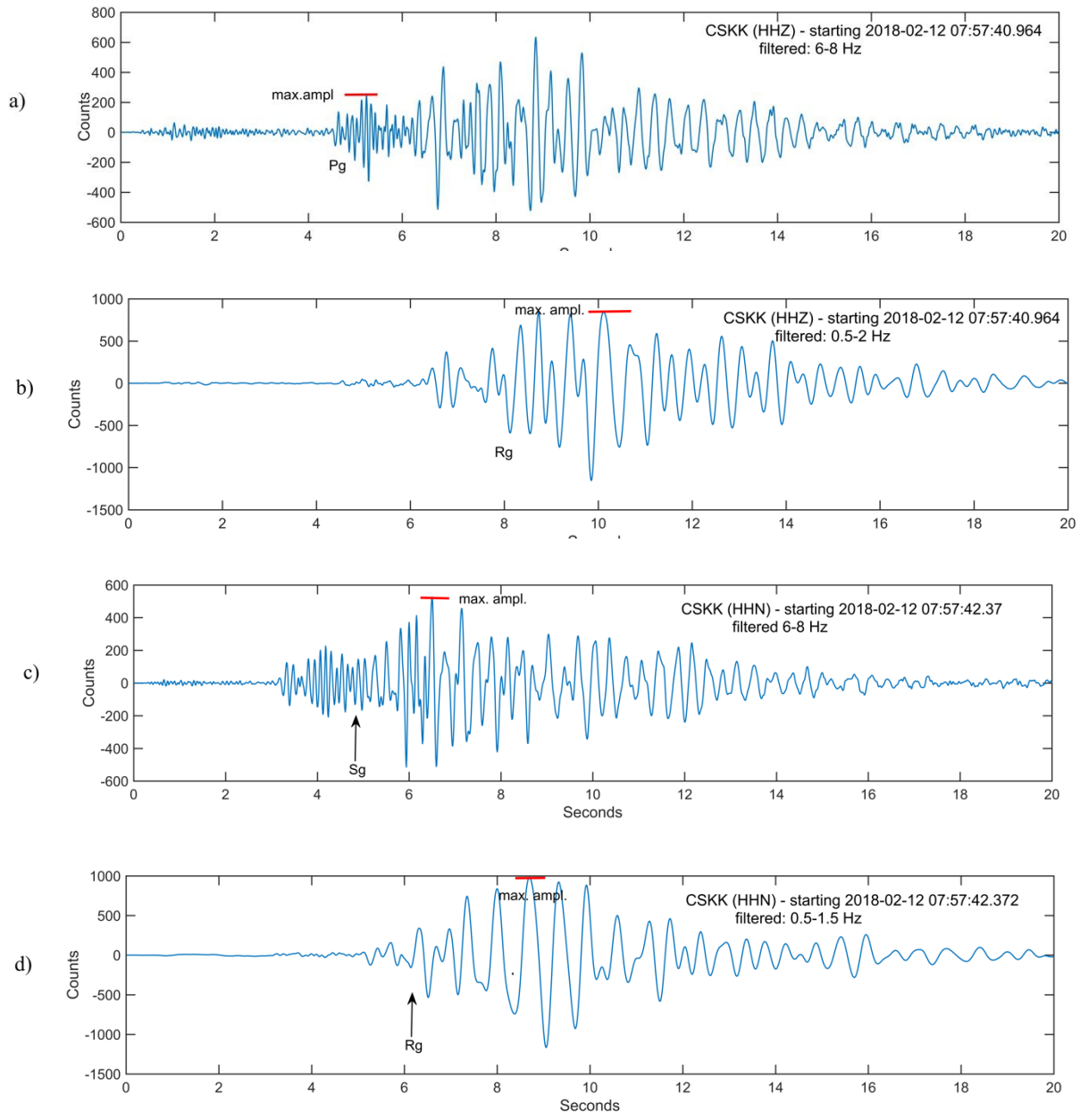

Figure 6. Maximum amplitudes are measured at different filtered bands a) P coda filtered 6–8 Hz; b) Rg filtered 0.5- 2 Hz; c) S coda filtered 6–8 Hz; d) S coda filtered between 0.5-1.5 Hz

Results

Below we describe the results of our discrimination analysis. **Figure 7** shows the logarithm of Rg/S amplitude ratio plotted against the logarithm of S/P amplitude ratio and the corresponding linear discrimination line between the earthquakes and explosions. Circles and triangles denote earthquakes and explosions in the training set, respectively, crosses and stars represent earthquakes and explosions in the validation set. The linear discrimination line separates 88.8% of the events in the training and validation set. **Table 2** shows the confusion matrix for the training and validation sets. The linear discrimination correctly classifies 92.4% of the events in the test set.

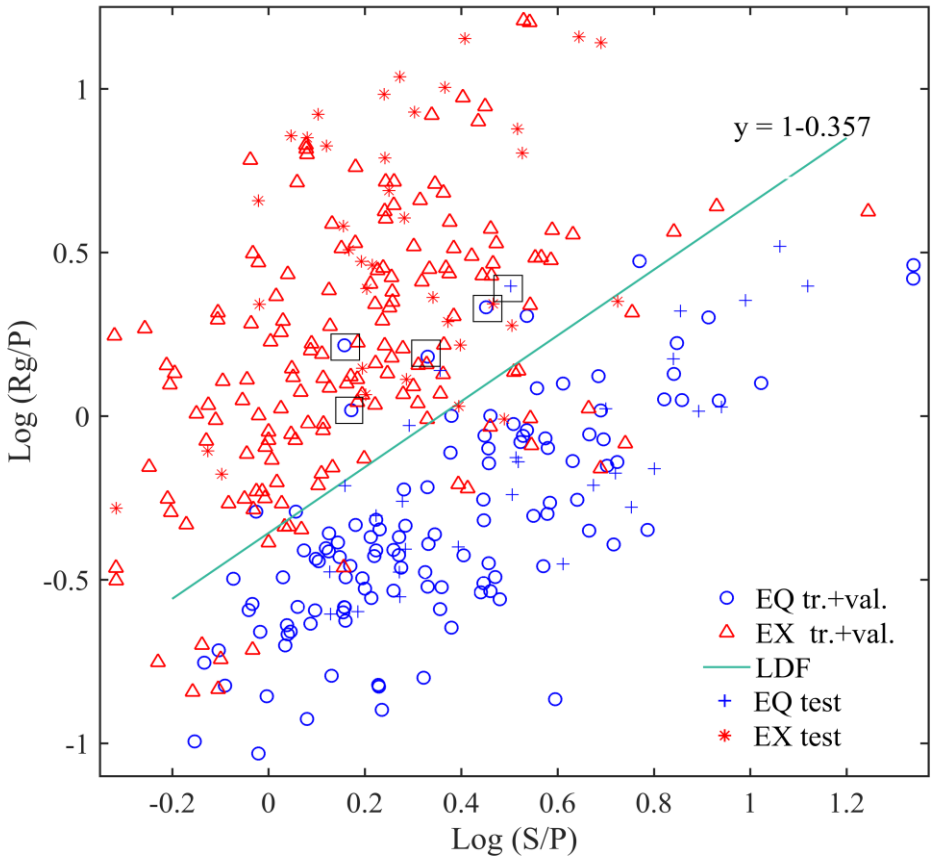

Figure 7. Peak amplitude ratio of Rg to P wave (vertical component) versus the peak amplitude ratio of S to P wave (filtered 6–8 Hz bands). Red triangles indicate the quarry blasts at Gánt, Iszkaszentgyörgy and Magyaralmás in the training and validation sets while the red stars show the test data set, respectively. The earthquakes training and validation sets that occurred in Mór Graben between 2017.01-2018.01 and Oroszlány (2011) aftershocks are indicated with blue circles. The earthquake test sets were indicated with blue crosses. The green line represents the linear discrimination line. Misclassified earthquakes are indicated with black squares.

Table 2. Correctly / incorrectly classified events in the training, validation and test data sets for phase amplitude ratios

Maximum phase amplitude ratios		**LDF EQ**	**LDF EX**	**Success rate**
Training + validation sets	**bulletin EQ**	110	8	88.8%
	bulletin EX	23	137	
Test set	**bulletin EQ**	27	2	92.4%
	bulletin EX	3	34	

Spectral properties

We measured the steepness of log power spectra between 1-10 Hz, and calculated the spectral ratios as the ratio of integrated spectral amplitudes in the 1- 10 Hz and 10-20 Hz frequency bands. The spectral parameters were measured using the GISMO MATLAB toolbox (Reyes and West 2011), These frequency bands indicate the spectral modulation of ripple-fired technique. **Figure 8** shows the spectral ratio against the steepness of power spectra between 1-10 Hz. The linear discrimination line separates 92.4% of events in the training set. **Table 3** shows the confusion matrix for the training and validation sets. The linear discrimination correctly classifies 95.5% of the events in the test data set.

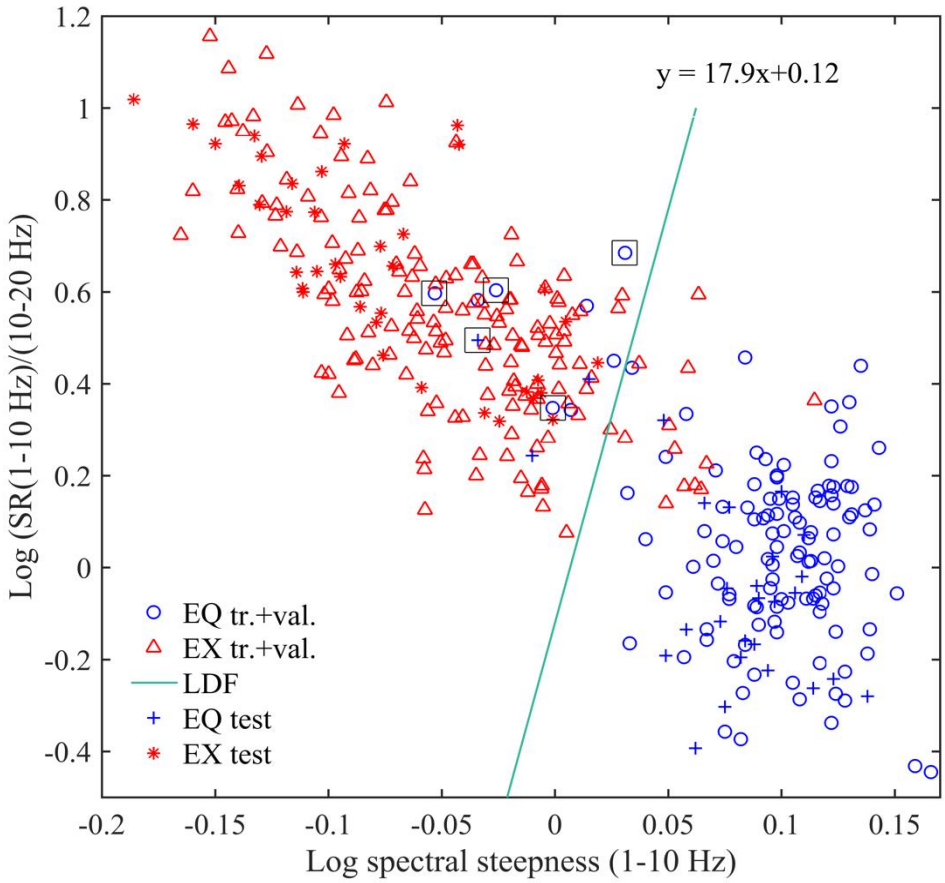

Figure 8. Spectral ratio versus steepness of power spectra. Spectral ratio values were calculated using the ratio of integrated spectral amplitudes in the selected lower (1-10 Hz) and higher frequency (10-20 Hz) bands.

Table 3. Correctly / incorrectly classified events in the training, validation and test data sets for spectral ratio and steepness

Spectral properties		LDF EQ	LDF EX	Success rate
Training + validation sets	**bulletin EQ**	110	8	92.4%
	bulletin EX	13	147	

Test set	**bulletin EQ**	26	3	95.5%
	bulletin EX	0	37	

Amplitude and spectral properties

Finally, we used the spectral steepness and maximum phase amplitude ratios together. **Figure 9** shows the steepness of power spectra plotted against the logarithm of peak amplitude ratio of S to P wave (filtered between 6–8 Hz). Note that the number of analyzed waveform and spectral parameters was different, because not all earthquakes and quarry blasts were suitable for reading all parameters. Here we only plotted those events for which both types of measurements were available. The linear discrimination line in this case separates 93.1% of the events. **Table 4** shows the confusion matrix for the training and validation sets. The linear discrimination correctly classifies 95.5% of the events in the test data set.

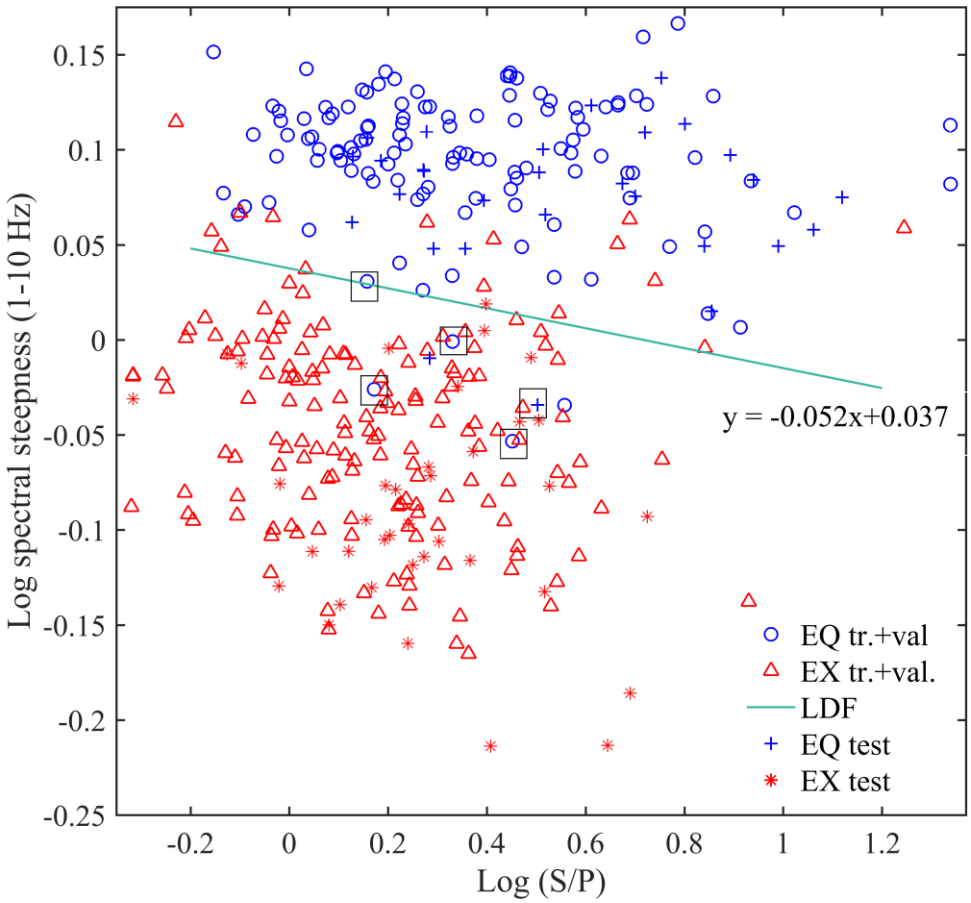

Figure 9. Steepness of power spectra plot versus peak amplitude ratio of S to P wave (filtered 6–8 Hz bands).

Table 4. Correctly / incorrectly classified events in the training, validation and test data sets for the steepness of power spectra and S/P amplitude ratio

Amplitude and spectral properties		LDF EQ	LDF EX	Success rate
Training + validation sets	**bulletin EQ**	114	4	93.1%
	bulletin EX	15	145	
Test set	**bulletin EQ**	27	2	95.5%
	bulletin EX	1	36	

Discussion and conclusions

The performed research has important implications for the discrimination of quarry blasts from the natural seismicity in the Mór Graben region within 25 km to the CSKK seismological station. We investigated three different discriminant options, the maximum amplitude ratios of Rg/P and S/P, the ratios of spectral steepness and spectral amplitude ratios, and finally the spectral steepness and the maximum amplitude ratio of S/P. The linear discrimination trained on the training and validation sets separated 88.8%, 92.4% and 93.1% success rate of the events, respectively. The linear discrimination performed similarly well on the test data set of 29 earthquakes and 37 quarry blasts, correctly classifying the events with 92.4% 95.6% and 95.5% success rate. There is no significant difference between the discrimination results of the 3 methods. Having a closer look at the earthquakes misclassified by the LDF method, five of them is the same ones that were misclassified using the amplitude and spectral parameters. These events are indicated with black open squares in Figure 7-8. Two of these events occurred at night, and the epicenters of two other events are within 5 km of the CSKK station. We performed waveform correlation using the GISMO Matlab toolbox (Reyes and West 2011) and analyzed 80-second-long seismograms filtered between 1-5 Hz. The correlation coefficient threshold was chosen to be 0.7. The explosions of different quarries formed different clusters. The waveforms belonging to individual quarries remained similar for over more than 4 years. However, none of the misclassified earthquakes proved to be similar to any quarry blasts. Therefore, these five events are most likely indeed earthquakes.

Among the main advantages of our method are that it can be used without the accurate knowledge of the epicenter, and linear discrimination method can be complemented with waveform cross-correlation. Note that the discriminants failed to correctly classify the quarry blasts from Magyaralmás, the closest mine 6.5 km away from CSKK. At such a close range the earthquakes and quarry blasts do not separate well in the frequency bands we used, and higher frequency ranges are already dominated by noise that would further hamper the discriminating power of the method.

Hence, the discriminants might be suboptimal at very close distances, but perform surprisingly well beyond 10 km epicentral distance.

Other possible limitation of our method is that the P/S ratio of earthquakes depends on the focal mechanism. Sometimes the earthquakes have frequency scalloping at low frequencies due to local effects similar to quarry blasts caused by ripple firing procedure.

The efficiency of our method can be increased creating a set of master events for individual quarries. This will allow us to run correlation detectors on past waveforms and identify explosions that were misclassified as earthquakes in the Hungarian National Bulletins. The contact with the mining districts can help to classify the events, because the separation of noisy and small magnitude events is a limitation of this method. The quarry blasts are ripple-fired in Vértes Mountains open pit blasts, consequently our event discrimination method is based on the recognition of ripple-firing modulations in the amplitude spectra. This method has only been tested for ripple-fired blasting technique, and we did not test for the single-fired quarry blasts.

Hedlin (1998) describes an automated discriminant that looks for delay-fire diagnostics in data. His method recognizes long-duration modulations in the binary spectrum and the algorithm estimates the time independence of the binary patterns by autocorrelation. His discriminant tests give misclassification probabilities, estimated with multivariate statistics, ranging from 0.5 to 3.5%. The algorithm that Arrowsmith et al. (2006) have developed is designed to exploit time-independent spectral modulations associated with delay-fired events too. In a drop-one test their method successfully identifies 97% of cast blasts and 84% of earthquakes. Kekovali et al. (2012) in the discrimination analysis between the earthquakes and mining blasts used S/P wave amplitude peak ratio, complexity, and spectral ratio. Their classification was obtained with acceptably high results of 99.6%.

We will test our methodology on further stations to assess the performance and portability of the discriminants. Based on our single station study, we conclude that our methodology may be able to discriminate between small, low magnitude earthquakes and quarry blasts at local epicentral distances between 10 and 50 km. In our case the neotectonic activity of the Mór Graben can be separated from anthropogenic events in the area, and the earthquake catalogue can be cleaned from the anthropogenic event facilitating better seismotectonic interpretation.

Acknowledgements

We thank the anonymous reviewer for the comments that helped us to improve the paper. This work was supported by the Hungarian National Research and Innovation Found Grant K128152.

References

Allmann B P, Shearer P M, Hauksson E (2008) Spectral discrimination between quarry blasts and earthquakes in southern California. BSSA 98(4):2073-2079

Arrowsmith S J, Arrowsmith M D, Hedlin M A H, Stump B. (2006) Discrimination of delay-Fired mine blasts in Wyoming using an automatic time-fr discriminanat. BSSA 96(6): 2368-2382

Bada G, Grenerczy Gy, Tóth L, Horváth F, Stein Seth, Cloetingh S, Windhoffer G, Fodor L, Pinter N, Fejes I (2007) Motion of Adria and ongoing inversion of the Pannonian Basin: Seismicity, GPS velocities, and stress transfer. Spec Pap Geol Soc Am 425:243-262

Baumgardt D R, Young G B (1990) Regional seismic waveform discrimination and case-based event identification using regional arrays. BSSA 80(6):1874-1892

Bondár I, Mónus P, Czanik C, Kiszely M, Gráczer Z, Wéber Z and the AlpArrayWorking Group (2018) Relocation of Seismicity in the Pannonian Basin Using a Global 3D Velocity Model. Seismol Res Lett 89:2284-2293

Budai T, Császár G, Csillag G, Fodor L, Kercsmár Zs, Kordos L, Selmeczi I (2008) Geology of the Vértes Hills. Explanatory book to the Geologycal Map of the Vértes Hills (1:50 000) - Magyar Állami Földtani Intézet, Budapest, 368.

Budakoğlu E, Horosan G (2018) Classification of seismic events using linear discriminant function (LDF) in the Sakarya region, Turkey. Acta Geophys 66:895–906

Douglas A, Hudson J A, Marshall P D, Young J B (1974) Earthquakes that look like Explosions. J Geophys Int 36:227-233

Fodor L, Kövér Sz (2013) Cenozoic deformation of the northern Transdanubian Range (Vértes Hills) Acta Petrol Mineral April 2013

Gitterman Y, Torild Van Eck (1993) High-frequency spectra of regional phases from earthquakes and chemical explosions. BSSA 83(4):1799-1812

Gráczer Z (ed.), Bondár I, Czanik Cs, Czifra T, Győri E, Kiszely M, Mónus P, Süle B, Szanyi Gy, Tóth L, Varga P, Wesztergom V, Wéber Z (2018) Hungarian National Seismological Bulletin 2017, Kövesligethy Radó Szeizmológiai Obszervatórium MTA CSFK GGI, Budapest 403 ISSN 2063-854X

Gráczer Z (ed.), Bondár I, Czanik Cs, Czifra T. Gyori E, Kiszely M, Kovács I J, Mónus P, Süle B, Szanyi Gy, Topa Zs, Tóth L, Varga P, Wesztergom V, Wéber Z (2019). Hungarian National Seismological Bulletin 2018, Kövesligethy Radó Szeizmológiai Obszervatórium, CSFK GGI, Budapest 593 ISSN 2063-854X

Gulia L (2010) Detection of quarry and mine blasts contamination in European regional catalogue. Nat Hazards V53:229-249

Hedlin M A, Minster J B, Orcutt J (1989) The time-frequency characteristics of quarry blasts and calibration explosion recorded in Kazakhstan, Geophys J Int 99:102-121

Hedlin M A (1998) A global test of a time-Frequency small-event discriminant. BSSA 88(4):973-988

Horasan G, Boztepe-Güney A, Küsmezer A, Bekler F, Öğütçü Z, Musaoğlu N (2009) Contamination of seismicity catalogs by quarry blasts: an example from Istanbul and its vicinity, Northwestern Turkey. J. Asian Earth Sci. 34:90–99

Joó I, Csepregi Sz (2007) A Móri-árok, továbbá a Bakony és a Vértes magassági irányú mozgásainak tanulmányozása. Geodézia és Kartográfia 59(4):3-8

Kafka A A (1990) Rg as a depth discriminant for earthquakes and explosions: a case study in new England. BSSA 80(2):373-394

Kekovali K, Kalafat D, Deniz P (2012) Spectral discrimination between mining blasts and natural earthquakes: Application to vicinity of Tunbilek mining area, western Turkey. Int J Phys Sci 7(35):5339-5352

Kim S G., Simpson D W, Richard P G (1994) High-frequency spectra of regional phases from earthquakes and chemical explosions. BSSA 84(5):1365-1386

Kiszely M, Győri E (2015) Separation of quarry blasts from the aftershock sequence of the Oroszlány (Hungary) January 29, 2011 ML = 4.5 Acta Geod Geoph Hung 50:97-107
Kintner J A, Cleveland K M, Ammon C J, Nyblade A (2020) Testing a Local-Distance Rg/Sg Discriminant Using Observations from the Bighorn Region, Wyoming. BSSA 110(2):727-741
Musil M, Pleŝinger A (1996) Discrimination between Local Microearthquakes and Quarry Blasts by Multi-Layer Perceptrons and Kohonene Maps. BSSA 86:1077-1090
Lomax A, Michelini A (2009) Mwpd: A Duration-Amplitude Procedure for Rapid Determination of Earthquake Magnitude and Tsunamigenic Potential from P Waveforms, Geophys J Int176:200-214, doi:10.1111/j.1365-246X.2008.03974.x
Pomeroy P W, Best J W, McEvilly T V, (1982) Test ban treaty verification with regional data - A review. BSSA 72:S89-S129.
Reyes C G, West M E, (2011) The Waveform Suite: A Robust Platform for Manipulating Waveforms in MATLAB, SRL 82(1):04-110
Taylor S R, Denny M D (1991) An analysis of spectral differences between NTS and Shagan River nuclear. J Geophys Res 96(4):6234-6245
Tóth L, Mónus P, Kiszely M, Trosits D (2018) Hungarian Earthquake Bulletin – 2017 GeoRisk, Budapest, pp 140 HU ISSN 1589-8326, doi:10.7914/SN/HM
Tóth L, Mónus P, Kiszely M, Trosits D (2019) Hungarian Earthquake Bulletin – 2018 GeoRisk, Budapest, pp 262 HU ISSN 1589-8326, doi:10.7914/SN/HM
Tóth L, Mónus P, Kiszely M, Trosits D (2020) Hungarian Earthquake Bulletin – 2019 GeoRisk, Budapest, pp 244 HU ISSN 1589-8326, doi:10.7914/SN/HM
Taylor S R, Sherman N W, Denny M D (1988) Spectral discrimination between NTS explosions and western U.S. earthquakes at regional distances. BSSA 78:1563-1579
Vargas M G, Rueda J, Blanco R M, Mezcua J (2017) A Real-Time Discrimination System of Earthquakes and Explosions for the Mainland Spanish Seismic Network, Pure Appl Geophys 174(1):213–228
Wiemer S, Baer M (2000) Mapping and removing quarry blasts events from seismicity catalogs. BSSA 90(2):525-530
Wüster J (1993) Discrimination of chemical explosions and earthquakes in Central Europe a case study. BSSA 83(4):1182-1212
Zeiler C, Velasco A A (2009) Developing local to regional explosion and earthquake discriminant. BSSA 99(1):24-35